Sustainable Food Technology

ROYAL SOCIETY OF CHEMISTRY

PAPER

View Article Online
View Journal | View Issue

Cite this: *Sustainable Food Technol.*, 2026, **4**, 482

Fabrication of blue emissive carbon dots using *Morinda citrifolia* fruit pulp for clodinafop and cypermethrin detection *via* fluorescence turn-off and enhancement mechanisms

Juhi Bhadresh Raval,[a] Vaibhavkumar N. Mehta,[b] Sanjay Jha,[b] Tae Jung Park [c] and Suresh Kumar Kailasa [*a]

The advancement in the field of fluorescence sensing requires the fabrication of superior nanoprobes that can quantify pesticides (clodinafop and cypermethrin) at trace levels for human health and environmental sustainability. Herein, blue emissive carbon dots (CDs) were fabricated using the ripe fruit pulp of *Morinda citrifolia* (*M. citrifolia*) as a biological ligand. The synthesized *M. citrifolia*-CDs possess blue fluorescence under UV light and exhibit excitation-independent emission behaviour at 340 nm across an excitation range of 300–400 nm, showing optimum emission intensity at 456 nm. The as-synthesized *M. citrifolia*-CDs show high water dispersibility and good stability for up to 100 days. The dynamic light scattering and zeta potential values of the as-synthesized CDs were found to be 7.17 nm and −37.3 mV, respectively, which showed remarkable changes after the addition of target pesticides. The introduction of clodinafop enhanced the fluorescence intensity, whereas the fluorescence was quenched by the addition of cypermethrin. The probe depicts remarkable sensitivity with limits of detection (LODs) of 0.079 and 0.028 μM for clodinafop and cypermethrin, respectively. The *M. citrifolia*-CDs acted as a selective nanoprobe for detection of clodinafop and cypermethrin and do not show any major fluorescence in the presence of chemical interfering agents. The as-synthesized CDs have been used for the fabrication of polymer thin films and fluorescent ink.

Received 7th July 2025
Accepted 8th October 2025

DOI: 10.1039/d5fb00364d

rsc.li/susfoodtech

Sustainability spotlight

The increasing use and presence of pesticides (clodinafop and cypermethrin) in agricultural products, food and environmental samples can cause a significant threat to human health, plants, ecology and export sustainability. Both pesticides (clodinafop and cypermethrin) are widely used in agriculture sectors to improve the yields of various crops. In view of this, a sustainable analytical strategy is essentially required to assay both pesticides in real samples. To meet green analytical chemistry, a fluorescent CD-based nanoprobe was fabricated from *Morinda citrifolia* fruit pulp and applied for sensing of both clodinafop and cypermethrin with different mechanisms. By enabling facile, rapid, selective assaying of clodinafop and cypermethrin in water, soil and vegetables, the developed fluorescent CDs derived from *Morinda citrifolia* fruit pulp hold great promise to assay both pesticides in real samples with minimized sample volumes and preparations. This work offers an eco-friendly and sustainable analytical strategy for monitoring clodinafop and cypermethrin in environmental and agri-food areas, promoting an efficient miniaturized analytical approach with minimized environmental impacts.

1. Introduction

Morinda citrifolia (*M. citrifolia*), recognized as Indian mulberry or noni fruit, from the family of Rubiaceae, is a tropical fruit native to Indonesia. The tremendous health benefits of noni fruit have gained widespread recognition and it is being widely cultivated in tropical and subtropical regions, exhibiting significant importance in both traditional and modern medicine. The fruit, leaves, and roots of the noni plant have all been widely used to cure a wide range of conditions, from infections to stomach problems. The noni fruit consists of an ovoid yellowish-white lumpy structure, which is made up of fused ripened ovaries. The noni fruit ranges in size from 10 to 12 cm, with an unpleasant yet strong odour when ripe, similar to butyric acid.[1–3] The pulp of noni fruit becomes gelatinous and juicy, with a dull white-yellowish appearance, and bitter as it ripens. The noni pulp is rich in bioactive compounds such as phenols, carotenoids, flavonoids, tannins, vitamin C, tocopherols, phytosterols, proteins, minerals, and polyunsaturated

[a]*Department of Chemistry, Sardar Vallabhbhai National Institute of Technology, Surat-395 007, Gujarat, India. E-mail: sureshkumarchem@gmail.com; skk@chem.svnit.ac.in*

[b]*ASPEE SHAKILAM Biotechnology Institute, Navsari Agricultural University, Surat, 395007, Gujarat, India*

[c]*Department of Chemistry, Research Institute of Chem-Bio Diagnostic Technology, Chung-Ang University, 84 Heukseok-ro, Dongjak-gu, Seoul 06974, Republic of Korea*

fatty acids.[4–6] These bio-active compounds can contribute to the antioxidant properties, leading to exploration of using it for various medical ailments. The noni fruit is also a valuable addition to the general diet as the pulp is rich in essential nutrients such as proteins, vitamins, carbohydrates, and minerals. The gelatinous fruit pulp has been widely used in traditional and modern recipes, despite its unpleasant odour and bitter taste, for its health benefits.[7] Due to the number of benefits the noni fruit provides, it has been widely employed as a food supplement, in the pharmaceutical industry and in the cosmetic industry. The therapeutic profile of the noni fruit and its sustainable cultivation make the noni fruit a crop for the future.

In order to explore its potentiality in fabricating fluorescent nanoprobes, *M. citrifolia* was used as a green precursor source for the synthesis of carbon dots (CDs). The ripe *M. citrifolia* pulp contains a mixture of phytochemicals, which would act as a rich carbon and heteroatom source for the fabrication of water-soluble fluorescent CDs. CDs derived from natural sources, including plant materials, are inherently biocompatible, eco-friendly, sustainable, and widely used for *in vivo* applications due to their low toxicity.[8–10] They align with the principles of green chemistry by reducing environmental impact and the complete minimization of hazardous chemicals. The usage of plant-extract-derived CDs offers several advantages, such as inexpensiveness, abundance of the precursor material, and sustainable development. The conventional methods are expensive and require typical organic ligands and toxic chemicals or acids for the synthesis of CDs, which in turn affect the environment. The fabrication of CDs from plant materials is cost-effective since plants are inexpensive and abundant and also less toxic to the environment.[11,12] Furthermore, plant extracts can provide natural variability for the fabrication of CDs with unique characteristics, enabling their applications in diverse fields of pharmacology, biology, and chemistry. Plant-mediated CDs have been widely utilized in the field of biomedical engineering, pharmaceuticals, and biological applications such as drug delivery, biosensing, bio-labelling, *etc.* In the present study, the two most widely used pesticides, *i.e.* clodinafop and cypermethrin, are employed as target analytes for their simultaneous detection using fluorescent CDs derived from ripe *M. citrifolia* pulp. In recent times, the use of pesticides has increased exponentially, and their residues in food and water raise concerns as they pose risks to animals, humans, and the environment. Clodinafop is a herbicide widely used in agriculture to control grass weeds in cereal crops, particularly wheat and barley, in the later stages of the crops. It has been reported to be used extensively in controlling grass weeds such as wild oats and foxtails. These weeds compete with the main crop for vital nutrients and basic requirements such as water and sunlight. The application of clodinafop has been reported to increase the grain quality and agricultural productivity by controlling the growth of unwanted plants and enhancing the main crop.[13,14] The careful management of clodinafop is required, as this herbicide can cause environmental pollution. Furthermore, clodinafop molecules do not get degraded and are washed off in larger water sources, contaminating them. While clodinafop poses low risks to non-target broadleaf plants, mammals, birds, and aquatic life, its use still requires management to prevent contamination. The recommended timings for clodinafop applications are crucial to minimise runoff and protect water sources.[15,16] On the other hand, cypermethrin is a generally employed synthetic pyrethroid insecticide known for its effectiveness against a broad range of pests.[17] It has been used widely for indoor pest control and agricultural fields. Every year, approximately 140 tons of cypermethrin are used on agricultural fields and 110 tons are used to manage indoor pests. This insecticide has properties of persistence in the soil for the long term, making it more effective against pests for a longer duration.[18] Cypermethrin disrupts the nervous system of insects by disrupting voltage-sensitive sodium channels, ultimately leading to death.[19,20] Cypermethrin is used extensively in agriculture and indoor pest control, posing health risks including neurological symptoms, immune system suppression, carcinogenic effects, suppression of antibody formation, and allergic reactions in humans. The harmful effects of cypermethrin make it necessary to detect it in food and soil matrices.[21]

The above studies demonstrated that the detection of the two pesticides in the field of agriculture is of utmost importance. Noticeably, in recent years the use of pesticides has increased ten times to manage weeds and pests and to enhance the quality and quantity of agricultural products. The extensive application of pesticides has led to environmental pollution and contamination of agricultural products and water sources.[22] It also poses a significant health risk to humankind with chronic illnesses due to insecticide-contaminated food consumption. The unrestricted employment of pesticides has led to the development of sensors that detect the minimum residue limits of pesticides in food, drinks, and soil, which is safe for the environment and human health.[23] It helps in enabling preventive measures to reduce the health risks associated with pesticide toxicity.

To the best of our knowledge, this is the first report for fabricating blue-emitting, uniformly dispersed CDs using *M. citrifolia* fruit pulp as a green source. The use of the green precursor eliminates toxic and hazardous chemicals. Various phytochemicals, such as phenols, carotenoids, flavonoids, tannins, tocopherols, phytosterols, and proteins, act as both a carbon source and heteroatom source, preventing the aggregation of CDs and resulting in improved fluorescence properties with enhanced stability. This method offers various advantages, such as being cost-effective, the use of a renewable carbon source, one-step reactions without the use of any chemical reagents, no major purification steps, and a dual-mode sensing strategy. In this study, we employed a sustainable yet effective method for fluorescence-based detection of cypermethrin and clodinafop *via* the turn-off and turn-on approach, respectively. The as-synthesized uniformly dispersed CDs were characterized using various techniques including fluorescence, UV-visible spectrophotometry for optical properties, and Fourier transform infrared (FT-IR) for understanding functional groups and interactions. Similarly, zeta potential, dynamic light scattering (DLS), field emission-transmission electron microscopy (FE-

TEM), X-ray photoelectron spectroscopy (XPS), X-ray diffraction (XRD) and life-time analysis were utilized for distinguishing various features and quenching mechanisms. The as-synthesized CDs were examined for their sensing applications on various pesticides, amongst which they showed remarkable selectivity towards clodinafop and cypermethrin. The highly dispersed *M. citrifolia*-CDs show aggregation-induced emission (AIE), in the presence of clodinafop, while depicting a remarkable reduction in the fluorescence intensity in the presence of cypermethrin. The probe shows limits of detection (LODs) of 0.079 and 0.028 μM and linear ranges of 0.025 to 1 and 0.05 to 2 μM for clodinafop and cypermethrin, respectively. The real sample analysis also shows good recovery rates with an RSD value of ≤2. The as-synthesized CDs from *M. citrifolia* pulp displayed promising fluorescence sensing applications for the detection of clodinafop and cypermethrin in food samples.

2. Experimental part

2.1. Chemicals and materials

M. citrifolia was collected from Navsari Agricultural University, Navsari, Surat. Various pesticides such as isoproturon, metsulfuron methyl, imazethapyr, clodinafop, pyrithiobac sodium, chlorothalonil, thiamethoxam, kresoxim methyl, lambda cyhalothrin, hexythiazox, cypermethrin, thiram, propiconazole, metribuzin, and mancozeb were received from Crop Life Science Ltd, Gujarat Insecticides Ltd, Super Crop Safe Ltd, Atul Ltd and Coromandel International Ltd. Water used in the entire experiment was purified using a Milli-Q water purification system. All the chemicals used were of analytical grade. All the glassware was cleaned with aqua regia and dried in a hot air oven and used after cleaning with acetone.

2.2. Instrumentation

The absorption data of *M. citrifolia*-CDs were measured using optical spectrophotometer Maya Pro 2000 from Ocean Optics, USA. A Cary Eclipse fluorescence spectrometer from Agilent Technologies, USA, was employed to record the emission and excitation spectral data of *M. citrifolia*-CDs. FT-IR spectrometer ALPHA II, Bruker, Germany, was utilized to record the functional groups of the *M. citrifolia*-CDs. To get the morphological structure of *M. citrifolia*-CDs, FE-TEM images were captured using an F200 JEOL microscope (Tokyo, Japan). The XPS and XRD analyses were carried out using a K-alpha+ by Thermo Fisher Scientific and new D8-Advance diffractometer by Bruker-AXS. A Horiba Scientific SZ-100V instrument was utilized for DLS and zeta potential measurements.

2.3. Quantum yield (QY) calculation

The QY of *M. citrifolia*-CDs was recorded using quinine sulphate (QS) as a reference standard. The absorbance spectra of the QS solution and *M. citrifolia*-CDs were measured using a UV-visible spectrophotometer. The emission and excitation spectral data were recorded for *M. citrifolia*-CDs and QS, respectively. For the calculation of QY, an integrated fluorescence *versus* absorbance area graph was plotted. The following equation was employed to calculate the QY of the *M. citrifolia*-CDs:

$$\mathrm{QY}_{M.\ citrifolia\text{-CDs}} = \mathrm{QY}_{M.\ citrifolia\text{-QS}} \times \frac{I_{M.\ citrifolia\text{-CDs}}}{I_{\mathrm{QS}}} \times \frac{{n_{M.\ citrifolia\text{-CDs}}}^2}{{n_{\mathrm{QS}}}^2} \times \frac{A_{\mathrm{QS}}}{A_{M.\ citrifolia\text{-CDs}}}$$

where "QS" in the subscript corresponds to the standard fluorescent QS dye, "*n*" denotes the refractive index of the solvent used in the solution, the absorption at the excitation wavelength is denoted by *A*, and integrated intensity/testing sample area is represented by *I*.

2.4. Fluorescence detection of the two pesticides

In this study, *M. citrifolia*-CDs were employed for the sensing of various pesticides. 1 mM solutions of several pesticides were prepared, specifically isoproturon, metsulfuron methyl, imazethapyr, pyrithiobac sodium, chlorothalonil, cypermethrin, thiamethoxam, kresoxim methyl, lambda-cyhalothrin, hexythiazox, and clodinafop. For the sensing experiment, 500 μL of each 1 mM analyte solution (pesticide) was separately combined with 1000 μL of *M. citrifolia*-CD solution in a vial and then vortexed for 120 s to ensure thorough mixing. The fluorescence spectra of the *M. citrifolia*-CDs and *M. citrifolia*-CDs with pesticides were obtained at an excitation wavelength of 340 nm. Upon analysis, notable changes were observed in the fluorescence spectra of *M. citrifolia*-CDs when clodinafop and cypermethrin were introduced. These changes in fluorescence emission suggest that *M. citrifolia*-CDs have the potential to act as effective fluorescent nanoprobes for the detection of clodinafop and cypermethrin pesticides.

2.5. Synthesis of thin polymer films and fluorescent ink from *M. citrifolia*-CDs

To fabricate the polymer film, 1 g of polyvinyl alcohol (PVA) was mixed with 50 mL of Milli-Q water and heated until a transparent solution was obtained. The solution was mixed with 5 mL of *M. citrifolia*-CD solution and stirred for 10 min for complete homogenization. The mixture was poured into a Petri plate and allowed to cool down at room temperature. The resulting thin films were observed under a UV-lamp for fluorescence, and images were captured. For the fluorescent ink application, a refillable pen was purchased from the local stationery. The pen was filled with the solution of *M. citrifolia*-CDs. The letters CD were calligraphed on the Whatman filter paper and air dried. The paper was then observed under a UV-lamp at 365 nm.

2.6. Analysis of pesticides in real samples

The *M. citrifolia*-CDs were employed for real-time application and are capable of assaying two real pesticide samples. As clodinafop and cypermethrin residues are found in river water, agricultural soil, and vegetables, we have taken samples from agricultural land, river water, and cabbage. The soil sample pretreatment was done by mixing 0.5 g of soil in double-distilled

water and sonicating for 15 min. The resultant mixture was then centrifuged at 10 000 rpm for 10 min, and the supernatant was spiked with various concentrations (0.1, 1.0, 10 and 100 μM) of cypermethrin and clodinafop for fluorescence analysis. River water samples were filtered using Whatman filter paper to remove insoluble substances and then spiked with different concentrations of pesticides, and their concentrations were estimated by measuring fluorescence spectra. For the cabbage sample, weighed portions were spiked with cypermethrin and clodinafop concentrations (0.1, 1.0, 10, and 100 μM) and kept in the dark for 24 h. Extraction was performed using a 1 : 1 ratio of water to methanol, and the solution was then sonicated for 20 min. It was subsequently filtered and the concentrations of target analytes were estimated by investigating fluorescence spectra.

3. Results and discussion

3.1. Characterization of *M. citrifolia*-CDs

For the fabrication of *M. citrifolia*-CDs, the pulp of ripe *M. citrifolia* fruit was mixed with an equal volume of Milli-Q water. A Teflon-lined stainless-steel vessel was used for the hydrothermal treatment and carbonized under pressure at 160 °C for 6 h. The resulting solution was then dialyzed to obtain a light-

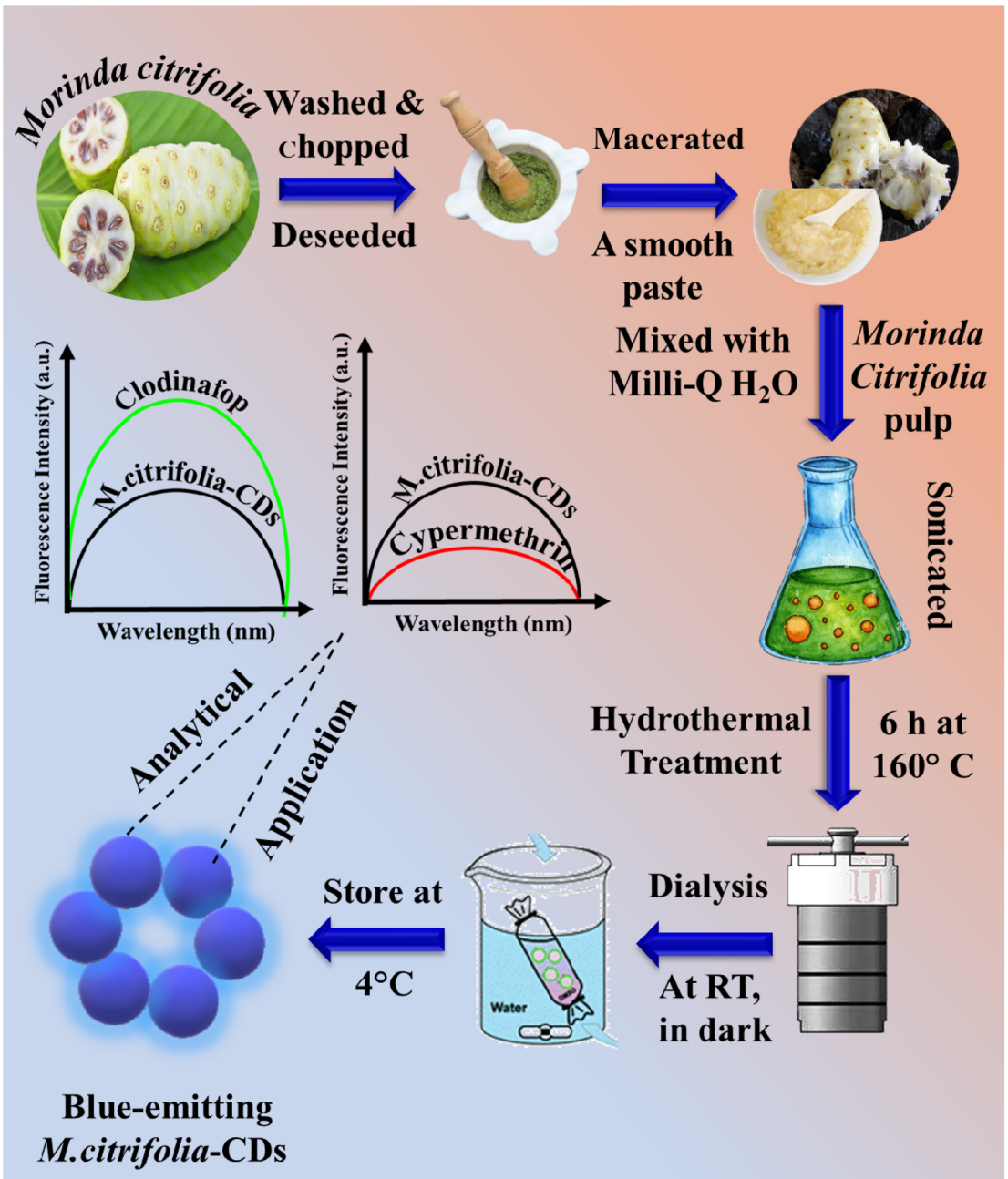

Scheme 1 Schematic depiction of the synthesis of blue-emitting *M. citrifolia* CDs and their sensing application for the detection of clodinafop and cypermethrin with different spectral variations.

yellow solution, revealing that the as-synthesized *M. citrifolia*-CDs are well dispersed with a uniform size. The formation of *M. citrifolia*-CDs is highly dependent on both the reaction time and temperature. These parameters were optimized to achieve the highest fluorescence intensity. As the carbonization temperature was increased from 100 to 160 °C, the fluorescence intensity of CDs increased noticeably; maximum intensity was noticed at 160 °C, but when the temperature was raised to 180 °C, the emission intensity decreased dramatically, which may be due to the structural deterioration or excessive carbonization as depicted in Fig. S1a in the SI. The influence of reaction time was also examined and the spectral data are shown in Fig. S1b in the SI, which revealed that the maximum fluorescence intensity was achieved at a reaction period of 6 h. While longer times resulted in a decrease in the emission, most likely as a result of surface passivation, group aggregation, or degradation, shorter times were inadequate for full carbonization. Consequently, it was found that 160 °C for 6 h produced the best fluorescence intensity. For the purification process, dialysis was applied to the as-synthesised *M. citrifolia*-CDs in order to eliminate unreacted by-products and to get a consistent size distribution. Using a dialysis membrane (usually with a molecular weight cut-off of ~12 000–14 000 Da), the dialysis was carried out for five hours against deionized water (Fig. S1c in the SI). This purification process was essential in getting rid of tiny molecule contaminants that may otherwise affect stability and optical qualities. Additionally, the regulated dialysis duration made it easier to concentrate CDs with somewhat homogeneous surface properties and sizes, which improved repeatability and contributed to consistent fluorescence behaviour in sensing applications. After that, the post-dialysis solution was collected and kept in a refrigerator for sensing applications and characterisation. A diagrammatic representation for the fabrication of *M. citrifolia*-CDs and their sensing applications for the detection of clodinafop and cypermethrin is depicted in Scheme 1.

To gain a deep insight into the characteristics of the *M. citrifolia*-CDs, various characterization techniques were employed. The optical properties were assessed using UV-vis spectroscopy and fluorescence spectroscopy. The *M. citrifolia*-CDs possess an absorption peak at 307 and 322 nm and an emission peak centered at 456 nm when excited at 350 nm (Fig. 1). The *M. citrifolia*-CDs appear light yellow in daytime and emit blue colour fluorescence under a UV lamp at 365 nm, as shown in the inset of Fig. 1. The *M. citrifolia*-CD UV-vis absorption spectra indicate n → π* transitions linked to C=O and C=N functionalities, respectively. These transitions imply the existence of surface groups that include nitrogen and oxygen, most likely derived from the pulp of *M. citrifolia*'s native phytoconstituents. Strong blue fluorescence was noticed in the emission spectra of *M. citrifolia*-CDs, which is due to surface passivation of CDs and surface defect states. A common property of many CDs generated from natural sources is excitation-independent fluorescence, which is facilitated by the surface energy traps introduced by heteroatom-rich groups (such as –OH, –COOH, and $–NH_2$) as depicted in Fig. S2 in the SI.

The FT-IR spectra are shown in Fig. S3 in the SI. The as-synthesized CDs exhibited characteristic bands that

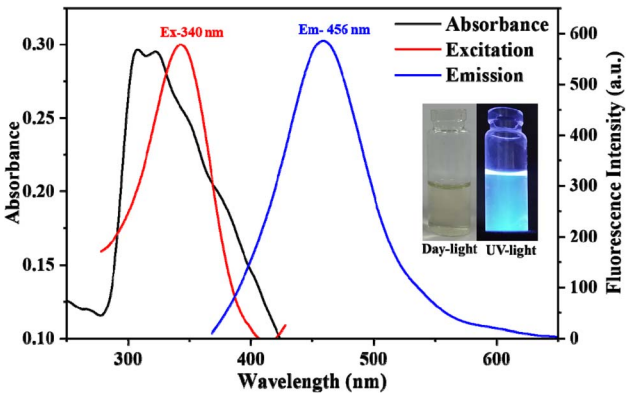

Fig. 1 Fluorescence spectra (excitation and emission) of *M. citrifolia*-CDs and the UV-visible spectrum of *M. citrifolia*-CDs (inset image of *M. citrifolia*-CDs under daylight and UV light (365 nm)).

corresponded to surface functional groups such as a broad O–H stretching band at around 3400 cm^{-1},[24] C–H stretching vibrations near 2920 and 2850 cm^{-1},[25] a sharp peak at ~1720 cm^{-1} attributed to C=O stretching of carboxylic groups,[26] aromatic C=C stretching near 1600 cm^{-1},[27,28] and strong C–O–C and C–O stretching vibrations between 1200 and 1000 cm^{-1}.[29,30] The structural and functional heterogeneity of the CDs is therefore confirmed by the combined UV-Vis and FTIR data, and the photoluminescence behaviour validates the successful tailoring of surface states that give rise to their optical features. The morphological structure of the *M. citrifolia*-CDs was found to be spherical, with a size distribution of 2.0 ± 0.4 nm, determined using FE-TEM as shown in Fig. 2a and b.

The hydrodynamic diameter of the as-synthesized CDs was correlated with FE-TEM, which was calculated to be 7.17 nm (Fig. S4a in the SI). The increase in the size of *M. citrifolia*-CDs is due to the hydration shell and surface functional groups present in the aqueous medium. In addition to improving water dispersibility, these functionalities also support surface charge and interparticle repulsion, two processes that are critical for preserving colloidal stability. The zeta potential value of −37.3 mV for *M. citrifolia*-CDs is indicative of its highly dispersive nature, and high electrostatic repulsion between the CDs is responsible for uniform dispersion and thereby preventing the aggregation of the fluorescent *M. citrifolia*-CDs (Fig. S4d in the SI). The long-term stability of *M. citrifolia*-CDs in suspension was further confirmed by visual inspection and repeated measurements conducted over 150 days (Fig. S5 in the SI), which revealed no apparent aggregation or sedimentation and only a slight decrease in the fluorescence intensity (after 100 days). The steric hindrance provided by functional groups and the electrostatic stabilization from surface charges are responsible for this steady fluorescence behaviour. For reproducibility and repeatability, the synthesis procedure for *M. citrifolia*-CDs was carried out at optimized parameters in three batches. The spectral data of different batches were studied and were recorded over 20 days, as depicted in Fig. S6a–c in the SI. The spectral data reveal that the emission characteristics of *M. citrifolia*-CDs exhibit good repeatability and reproducibility,

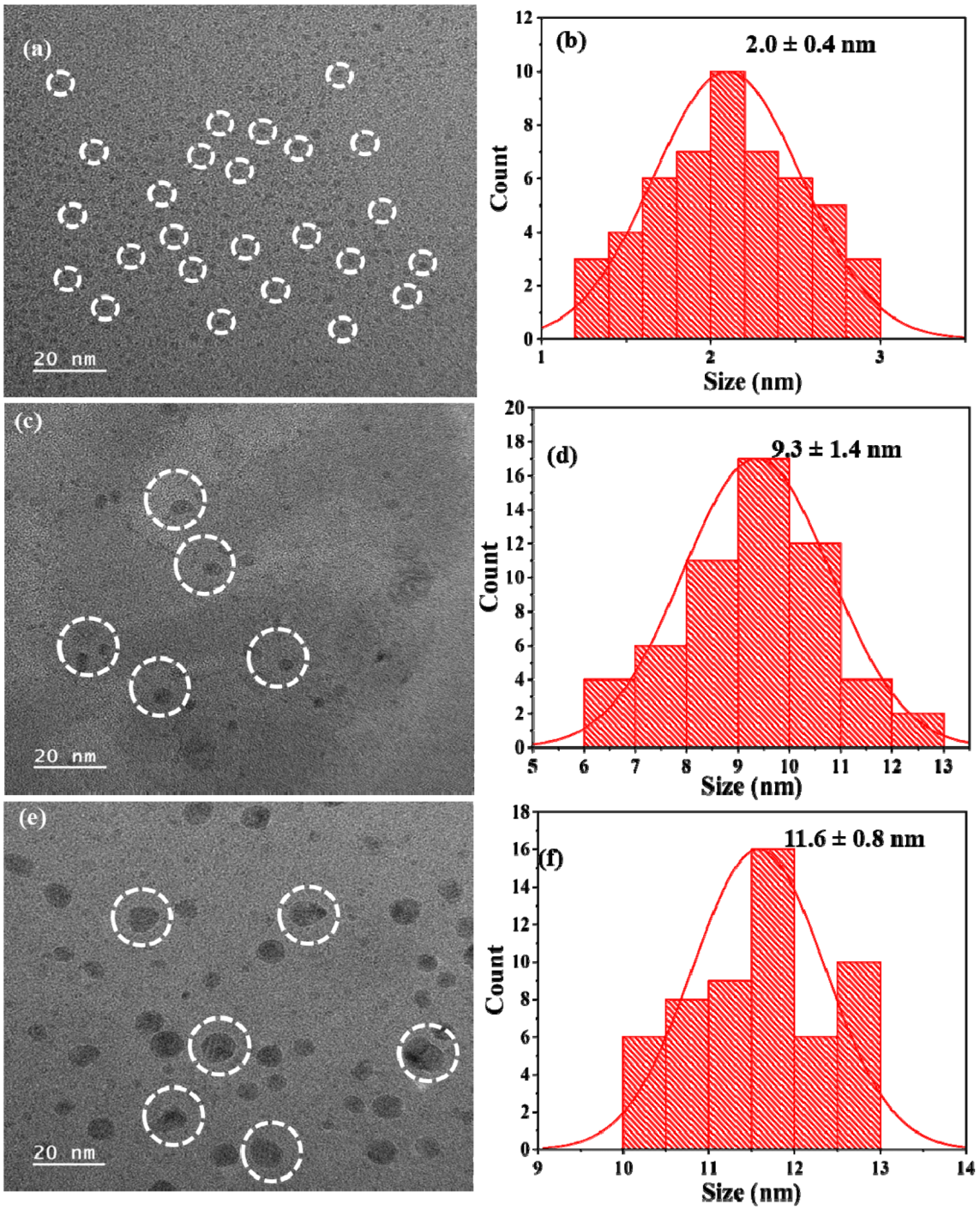

Fig. 2 (a) FE-TEM image of *M. citrifolia*-CDs, (b) histogram plotted for the average size of *M. citrifolia*-CDs, (c) FE-TEM image of *M. citrifolia*-CDs + clodinafop, (d) histogram plotted for the average size of *M. citrifolia*-CDs + clodinafop, (e) FE-TEM image of *M. citrifolia*-CDs + cypermethrin, and (f) histogram plotted for the average size of *M. citrifolia*-CDs + cypermethrin.

with no significant change in fluorescence intensity observed across all three batches.

The elemental composition of *M. citrifolia*-CDs was determined using XPS (Fig. 3). The full scan survey spectrum (Fig. 3a) displays two prominent peaks corresponding to C 1s and O 1s at binding energies of 286.0 and 534.6 eV, respectively.[31] The O 1s spectrum (Fig. 3b) exhibits a peak at 534.6 eV, which is attributed to C–OH groups. The N 1s spectrum (Fig. 3c) shows a peak at 401.1 eV, indicative of the presence of C–N–H groups in the CDs.[32,33] Additionally, in the C 1s XPS spectrum (Fig. 3d), two distinct peaks were observed, representing C in C–C/C–O bonds at 286.21 eV and C=O bonds at 288.06 eV.[34,35] The XRD analysis was performed to determine the nature of *M. citrifolia* pulp and the as-synthesized CDs. The *M. citrifolia* fruit pulp XRD analysis reveals broad diffraction peaks at around 21.8°, 30.08°, and 44.70° with no crystalline order and an amorphous nature, as

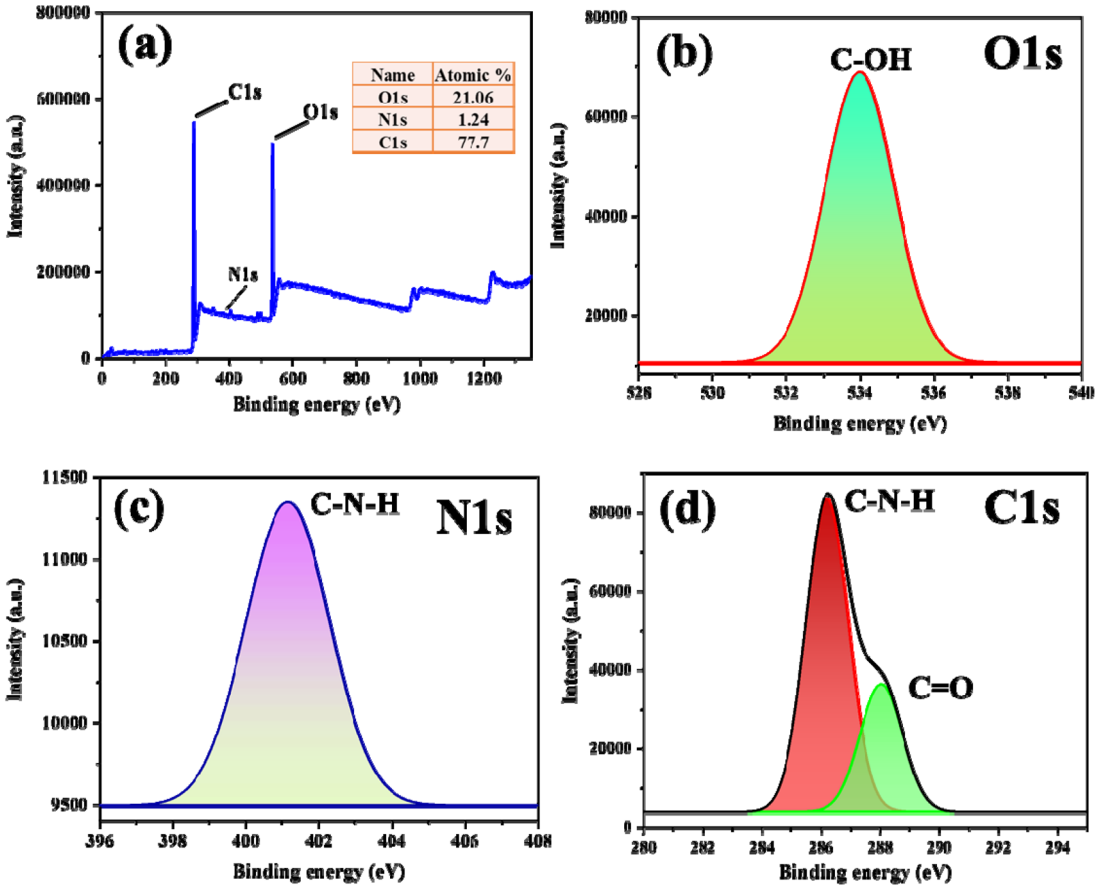

Fig. 3 XPS analysis of *M. citrifolia*-CDs, (a) survey spectrum with element percentage, (b) O1s (c) N1s and (d) C1s.

depicted in Fig. S7a in the SI. The XRD analysis of *M. citrifolia*-CDs displays various angles at $2\theta = 14.83°$, 21.8°, 28.2°, 30.08°, 40.51°, suggestive of broad and slightly sharp diffraction peaks, as shown in Fig. S7b in the SI. The peaks are suggestive of the amorphous nature of the *M. citrifolia*-CDs. The broad peaks at around 21.8° are also suggestive of disordered carbon atoms and graphitic lattices in the structure of as-synthesized *M. citrifolia*-CDs.[36–38] Thus, while comparing both, it is evident that the precursor molecules have undergone structural transformation into a carbon-rich structure with more disordered graphitic lattices.

3.2. Fluorescence sensing of pesticides

To investigate the sensing applications of the as-synthesized *M. citrifolia*-CDs towards various pesticides, we examined their sensing ability with a range of pesticides, including isoproturon, metsulfuron methyl, imazethapyr, pyrithiobac sodium, chlorothalonil, cypermethrin, thiamethoxam, kresoxim methyl, lambda-cyhalothrin, hexythiazox, and clodinafop. The fluorescence spectra of the *M. citrifolia*-CDs were recorded in the presence of each pesticide, as depicted in Fig. 4a. The change in the fluorescence behaviour under UV light at 365 nm is shown in Fig. 4b. The results demonstrated significant changes in the fluorescence emission intensity upon the addition of clodinafop and cypermethrin. Specifically, the fluorescence intensity was quenched by 80% in the presence of cypermethrin, indicating a strong interaction between the *M. citrifolia*-CDs and target pesticide (cypermethrin). In contrast, the fluorescence intensity was enhanced in the presence of clodinafop, suggesting an AIE type of interaction that results in fluorescence enhancement. These observations indicate that the as-synthesized *M. citrifolia*-CDs can function effectively as fluorescent sensors for pesticide detection. The fluorescence spectra recorded in the presence of various pesticides and the remarkable changes observed in the spectral data in the presence of clodinafop and cypermethrin make them promising candidates for the sensing of target pesticides in food safety and environmental monitoring. To check the reproducibility of the developed method, three batches of *M. citrifolia*-CDs were employed for the detection of clodinafop and cypermethrin. The spectral data are shown in Fig. S6d–f, indicating that the as-synthesized probe shows good precision and accuracy for assaying of the two pesticides in all three batches.

3.3. pH study

Fluorescence sensing ability of the as-synthesized CDs was evaluated under different pH conditions using phosphate-buffered saline (PBS). The *M. citrifolia*-CD solution was added to various pH solutions (2 to 12) to assess its stability and sensing performance. The fluorescence intensity of the probe

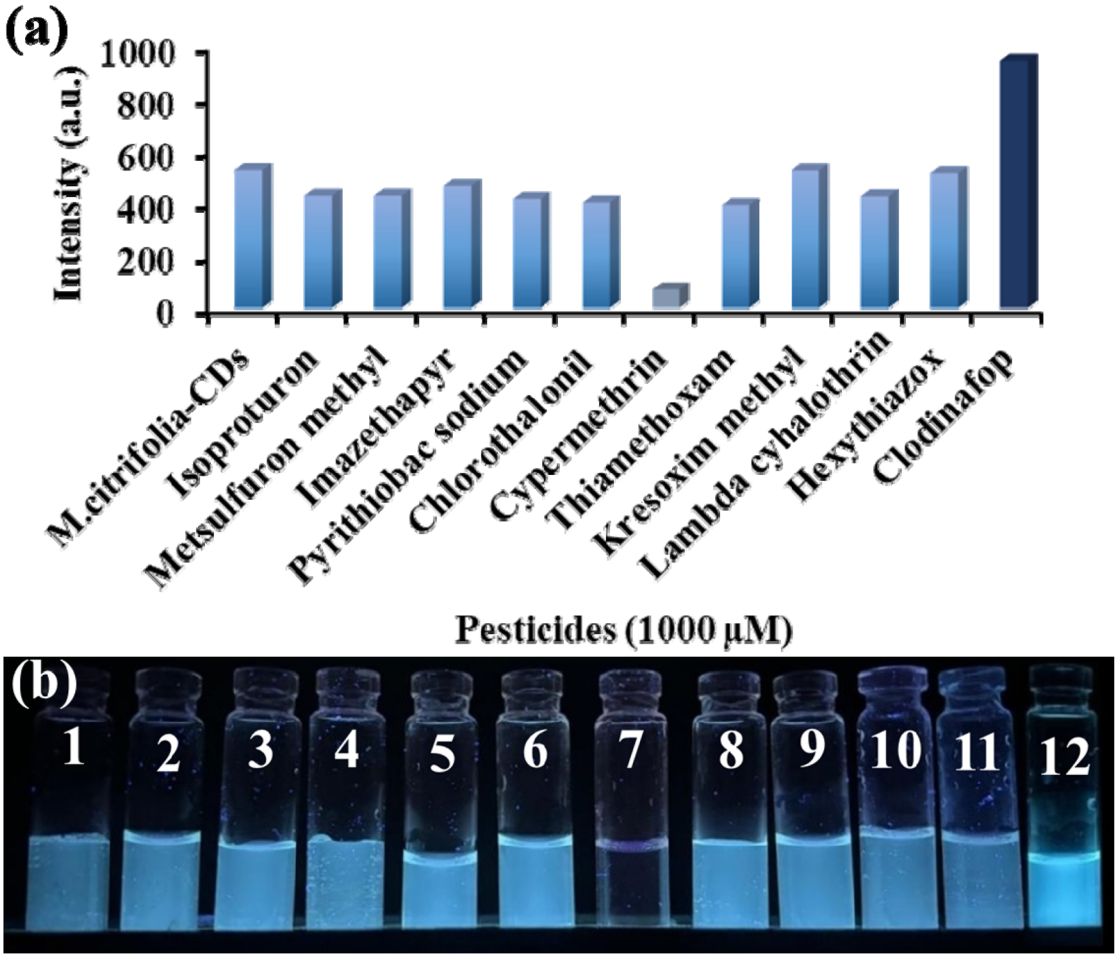

Fig. 4 (a) Fluorescence emission spectra of *M. citrifolia*-CDs at an emission wavelength of 456 nm with the addition of various pesticide (isoproturon, metsulfuron methyl, imazethapyr, pyrithiobac sodium, chlorothalonil, cypermethrin, thiamethoxam, kresoxim methyl, lambda cyhalothrin, hexythiazox, and clodinafop) solutions. (b) Variation in the fluorescence intensities of *M. citrifolia*-CD solutions in the presence of different pesticides under a UV lamp at 365 nm (1 – *M. citrifolia*-CDs, 2 – isoproturon, 3 – metsulfuron methyl, 4 – imazethapyr, 5 – pyrithiobac sodium, 6 – chlorothalonil, 7 – cypermethrin, 8 – thiamethoxam, 9 – kresoxim methyl, 10 – lambda cyhalothrin, 11 – hexythiazox, and 12 – clodinafop).

remains stable, showing no spectral variation, suggesting that across the tested pH range of 2 to 12, the probe does not disintegrate and exhibits the same fluorescence properties as shown in Fig. S8a, SI. To explore the sensing properties further, the synthesized probe was exposed to a similar pH range (2 to 12) in the presence of clodinafop and cypermethrin. The spectral data suggest that there was no significant change in the enhancement and quenching of the fluorescence intensity across the tested PBS pH range by clodinafop and cypermethrin, respectively (Fig. S8b and c, SI). These findings suggest that the as-synthesized *M. citrifolia*-CDs remain unaffected over a wide spectrum of PBS pH, maintaining their fluorescence stability and functional integrity. This characteristic of *M. citrifolia*-CDs makes them fit for a number of applications in biological and environmental systems.

3.4. Sensing mechanism

To elucidate the sensing mechanism of *M. citrifolia*-CDs with clodinafop and cypermethrin, different characterization studies were performed. The FT-IR spectra of *M. citrifolia*-CDs with clodinafop show a change in the intensity and spectral shifts in the region of O–H bending and C=O stretching, which are indicative of the interactions between carboxyl and hydroxyl groups of *M. citrifolia*-CDs with hydroxyl and ester functionalities of clodinafop. Minimal spectral changes were observed in the C=C regions which are due to the π–π stacking interactions between the phenoxy moiety of clodinafop and aromatic groups present on the surface of *M. citrifolia*-CDs. In accordance with the changes observed in the FT-IR spectra, the *M. citrifolia*-CDs bind with clodinafop *via* dipole–dipole interactions, π–π stacking, and non-covalent bonding. On the other side, the FT-IR data of cypermethrin with *M. citrifolia*-CDs show remarkable changes in the O–H stretching region, broadening of the C–O–C region, and the C=O ester band. The ester and nitrile groups of cypermethrin bind with the hydroxyl groups of *M. citrifolia*-CDs *via* non-covalent binding. The non-polar domains of the *M. citrifolia*-CDs can interact with the alkyl-halide chains of cypermethrin by van der Waals interactions. The aromatic ring

of cypermethrin and the aromatic domains of CDs suggest weak π–π stacking, resulting in no major spectral shifts. Collectively, the data confirm that both pesticides interact non-covalently with the surface functionalities of *M. citrifolia*-CDs through a mixture of π–π stacking, hydrogen bonding, dipole interactions, and hydrophobic forces, enabling their potential utility in pesticide detection applications (Fig. S3 in the SI). The lifetime analysis was performed to measure the fluorescence decay time of the probe. It was observed that the decay times of *M. citrifolia*-CDs, *M. citrifolia*-CDs + clodinafop, and *M. citrifolia*-CDs + cypermethrin were 0.36, 0.35, and 0.34 ns, respectively. The decay time analysis is shown in Fig. 5. The *M. citrifolia*-CDs show static quenching in the presence of cypermethrin, which was validated with a positive curvature of the Stern–Volmer plot (Fig. 7b).[39] The FT-IR data also suggest the formation of π–π stacking, hydrogen bonding, and van der Waals interaction, which form a non-fluorescent complex before excitation, hence indicative of static quenching. The lifetime decay value of *M. citrifolia*-CDs in the presence of clodinafop is nearly unchanged, suggesting that in the presence of clodinafop, the electron recombination pathway is not altered. The negligible change in the decay time rules out the possibility of dynamic quenching. The fluorescence intensity of *M. citrifolia*-CDs is enhanced in the presence of clodinafop. This enhancement is due to AIE; the clodinafop molecules, when interacting with *M. citrifolia*-CDs, reduce the density of non-radiative electron traps responsible for energy dissipation and in turn increase the probability of radiative recombination leading to an increase in the fluorescence intensity.[40] The clodinafop molecules reduce the intramolecular rotations and vibrations, thereby strengthening the π–π conjugation within the carbon core. Therefore, the fluorescence enhancement in the presence of clodinafop is due to AIE, and the fluorescence quenching of *M. citrifolia*-CDs in the presence of cypermethrin is due to static quenching.

To identify the morphological changes of the synthesized *M. citrifolia*-CDs with pesticides, FE-TEM images were examined. The average diameters of the as-synthesized *M. citrifolia*-CDs, *M. citrifolia*-CDs + clodinafop, and *M. citrifolia*-CDs + cypermethrin were found to be 2.0 ± 0.4, 9.3 ± 1.4 and 11.6 ± 0.8 nm, respectively (Fig. 2c–f). With the addition of cypermethrin and clodinafop, the *M. citrifolia*-CDs tend to aggregate and show an increase in size due to the interactions of clodinafop and cypermethrin with *M. citrifolia*-CDs. The hydrodynamic diameter of the *M. citrifolia*-CDs was found to be 4.9 nm, while after the addition of clodinafop and cypermethrin, the hydrodynamic diameter was increased to 24.29 and 31.01 nm, respectively as depicted in Fig. S4b and c in the SI. The increase in size is due to the adsorption of clodinafop and cypermethrin on *M. citrifolia*-CD surfaces. The zeta potential value of *M. citrifolia*-CDs is −37.3 mV, indicating the high stability of the synthesized CDs. The decrease in the value of zeta potential, *i.e.*, −4.4 mV, after the addition of clodinafop is due to the electrostatic interaction between the probe and analyte (Fig. S4e in the SI). Also, the addition of cypermethrin has reduced the negative charge of the *M. citrifolia*-CDs, and the zeta potential value was found to be −2.5 mV (Fig. S4f in the SI). The reduction in the zeta potential value is due to the electrostatic neutralization *via* the binding of the pesticide on the surface of the *M. citrifolia*-CDs.

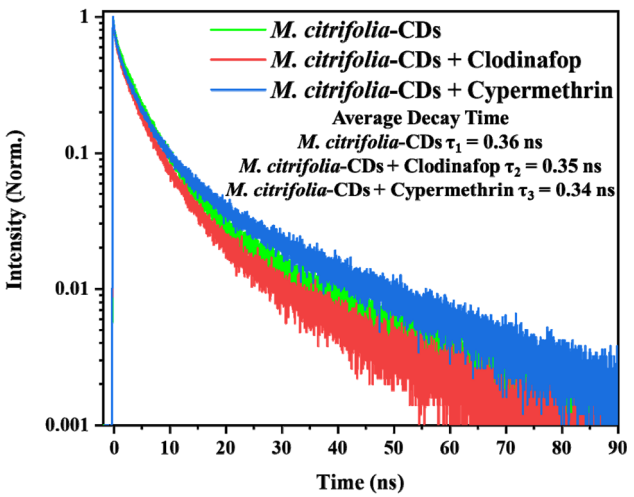

Fig. 5 (a) Lifetime analysis of *M. citrifolia*-CDs,*M. citrifolia*-CDs + clodinafop, and *M. citrifolia*-CDs + cypermethrin.

3.5. Sensitivity study

By adding different concentrations of clodinafop (0.10 to 1000 μM) and cypermethrin (0.05 to 1000 μM), the intensity of *M. citrifolia*-CDs was recorded at an excitation wavelength of 350 nm. The emission intensity is directly proportional to the concentration of analytes (clodinafop and cypermethrin). Fig. 6a suggests that the intensity of *M. citrifolia*-CDs (I/I_0) at 456 nm increased in proportion to the concentration of clodinafop. A calibration graph was plotted for emission intensity (I/I_0) against the concentration of clodinafop (Fig. 6b and c). From the linear regression, the correlation coefficient, R^2 was found to be 0.9863, where I is emission intensity with clodinafop and I_0 is emission intensity in the absence of clodinafop. The probe shows a detection limit of 0.079 μM, with a linear range of 0.10 to 1.0 μM. Fig. 6d shows a photographic image of *M. citrifolia*-CDs under 365 nm UV light, suggesting progressive enhancement in fluorescence with an increasing concentration of clodinafop. On the other hand, with the addition of cypermethrin, the intensity of the as-synthesized CDs decreased proportionally (Fig. 7a). The Stern–Volmer experiment was carried out and plotted as a function of I_0/I and the concentration of cypermethrin. The positive curvature of the Stern–Volmer plot confirms static quenching between *M. citrifolia*-CDs and cypermethrin (Fig. 7b).[39] The linear decrease in the intensity of *M. citrifolia*-CDs exhibits a correlation coefficient (R^2) value of 0.9987, as depicted in the calibration curve I_0/I plotted between I (emission intensity with cypermethrin) and I_0 (emission intensity in the absence of cypermethrin) (Fig. 7c). The decrease in the fluorescence intensity under the UV lamp is shown in Fig. 7d. The probe exhibits a LOD of 0.028 μM with a linear range of 0.05 to 2.0 μM. The comparative analyses of the present study with the other reported methods for the detection of clodinafop and cypermethrin are shown in SI Tables S1 (clodinafop)[41–46] and S2 (cypermethrin).[47–54]

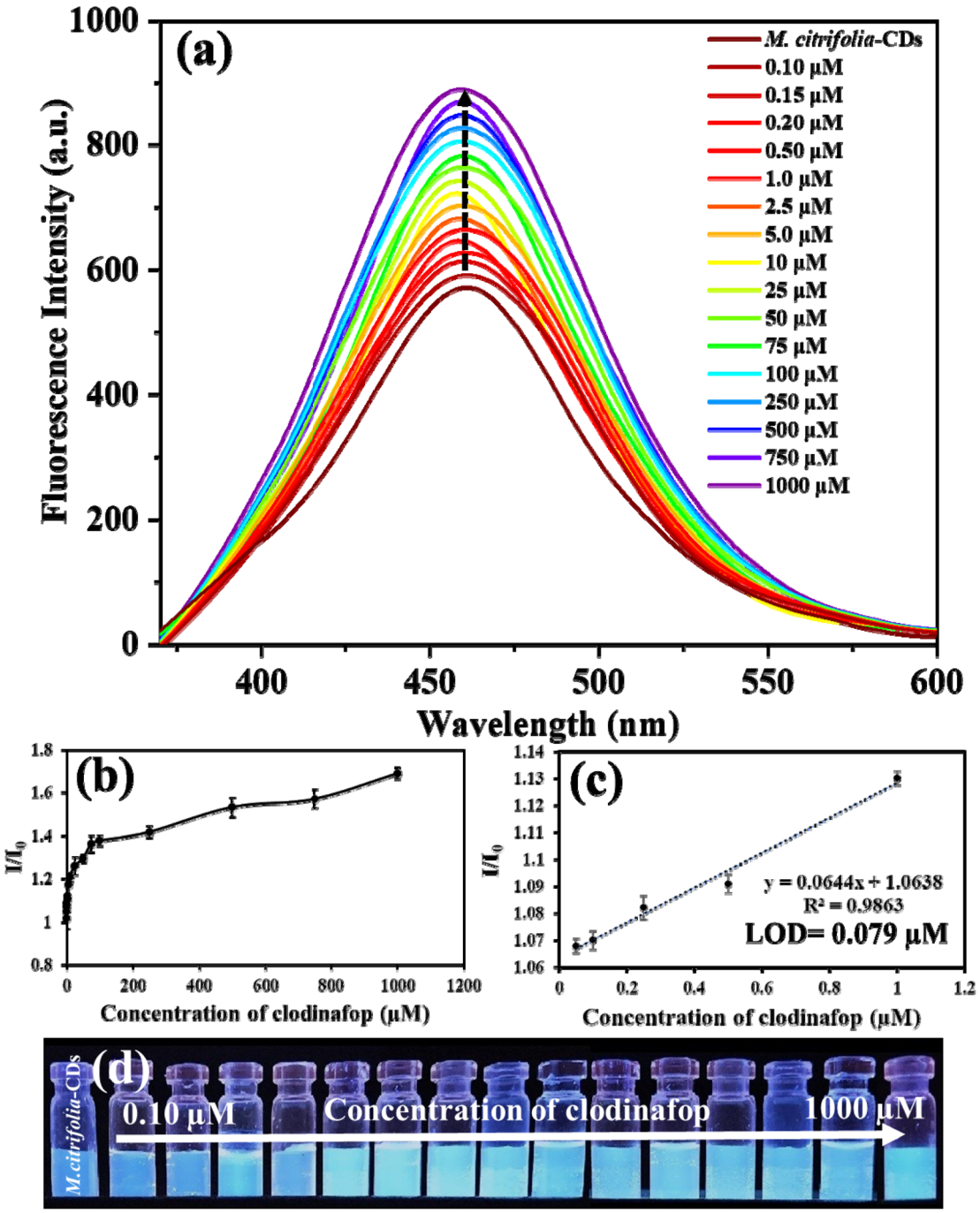

Fig. 6 (a) Fluorescence emission spectra of *M. citrifolia*-CDs after addition of different concentrations of clodinafop (0.10–1000 µM) solutions. (b and c) Calibration curve plotted between I/I_0 and concentrations of clodinafop with a linear range of 0.1–1.0 µM. (d) The photographic representation of fluorescence changes in *M. citrifolia*-CDs with an increasing concentration of clodinafop under a UV lamp at 365 nm.

3.6. Interference study of *M. citrifolia*-CDs

The selectivity of *M. citrifolia*-CDs, in the presence of other chemical interfering species, *i.e.*, with anions and cations (Cu^{2+}, Na^{+}, Ni^{2+}, Co^{2+}, K^{+}, Br^{-}, SO_4^{2-}, and Cl^{-}, 1000 µM), biomolecules (L-cysteine, asparagine, ascorbic acid, and glucose, 1000 µM), and pesticides (thiram, propiconazole, metribuzin, and mancozeb, 1000 µM), on the fluorescence emission of *M. citrifolia*-CDs was investigated in the presence and absence of clodinafop. Similarly, potential interferents, such as mixtures of cations and anions (Pb^{2+}, Mg^{2+}, Mn^{2+}, Ca^{2+}, Cu^{2+}, Br^{-}, SO_4^{2-}, and Cl^{-} 1000 µM), biomolecules (L-leucine, L-tryptophan, glucose, and thiamine; 1000 µM), and pesticides (terbufos, quinalphos, sulfosulfuron, and hexaconazole, 1000 µM) were also tested with cypermethrin to investigate the selectivity of the probe. The emission intensity of *M. citrifolia*-CDs remains unchanged with the addition of the above chemical species in the absence of clodinafop and cypermethrin (SI Fig. S9a and S10a). However, with the addition of clodinafop, the

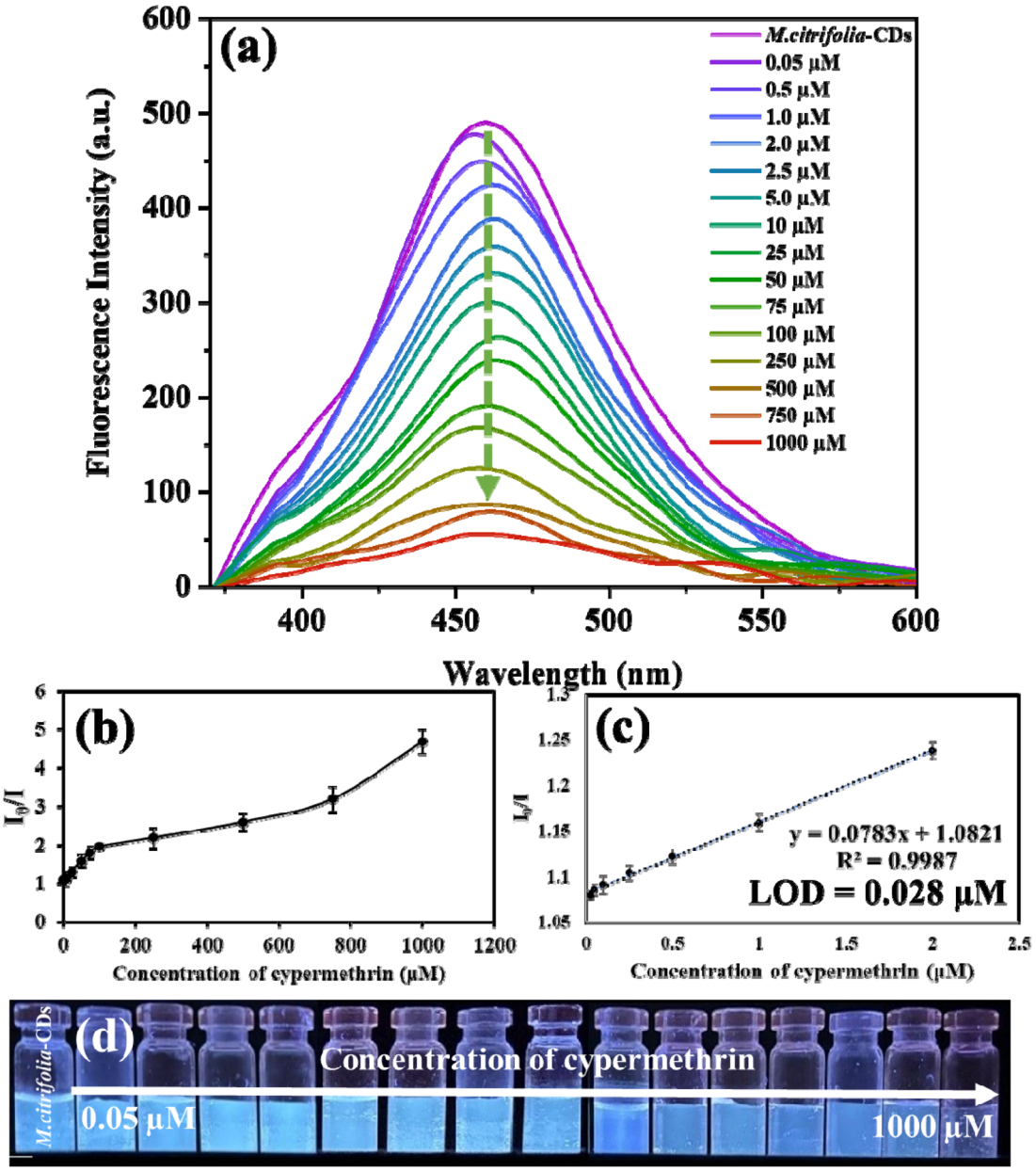

Fig. 7 (a) Fluorescence emission spectra of *M. citrifolia*-CDs after addition of different concentrations of cypermethrin (0.05–1000 µM) solutions. (b) Stern–Volmer plot between I_0/I and concentrations of cypermethrin. (c) Calibration curve plotted between I_0/I and concentrations of cypermethrin. (d) The photographic representation of fluorescence changes in *M. citrifolia*-CDs with an increasing concentration of cypermethrin under a UV lamp at 365 nm.

fluorescence intensity is enhanced, while in the presence of cypermethrin it is quenched (SI Fig. S9b and S10b). These suggest that *M. citrifolia*-CDs only show changes in the presence of clodinafop and cypermethrin, being highly selective in nature. In addition to this, a cross-interference study was carried out in the presence of different ratios of clodinafop and cypermethrin (SI Fig. S11a and b). The spectral data reveal that cypermethrin exerts a stronger influence on the fluorescence quenching of *M. citrifolia*-CDs due to strong electron-withdrawing groups such as the –CN moiety, halogenated aromatics, and ester functionalities. In contrast, clodinafop possesses aromatic rings that interact with the *M. citrifolia*-CDs *via* π–π stacking and hydrogen bonding, resulting in surface passivation on the synthesized CDs. Therefore, when in a mixture of clodinafop and cypermethrin, cypermethrin shows major quenching due to multiple electron-withdrawing groups hindering the binding of clodinafop and in turn decreasing the enhancement of fluorescence intensity.

3.7. Polymer thin films and fluorescent ink using *M. citrifolia*-CDs

The stable fluorescence properties, high dispersibility, and optical transparency of *M. citrifolia*-CDs can be utilized for fabrication of polymer thin films and fluorescent ink.[55] The

Table 1 Analysis of clodinafop in various environmental samples using *M. citrifolia*-CDs as a probe

Sample	Added concentration (μM)	Found concentration (μM)	Recovery (%)	RSD (%) ($n = 3$)
River water	0.1	0.099	99.85	0.138
	1.0	0.998	99.81	0.055
	10	9.817	98.17	0.247
	100	98.90	98.90	0.372
Agricultural soil	0.1	0.099	99.36	0.168
	1.0	0.997	99.72	0.088
	10	9.950	99.50	0.340
	100	97.36	97.36	0.275
Cabbage	0.1	0.099	99.71	0.180
	1.0	0.995	99.54	0.150
	10	9.901	99.01	0.314
	100	97.20	97.20	0.263

Table 2 Analysis of cypermethrin in various environmental samples using *M. citrifolia*-CDs as a probe

Sample	Added concentration (μM)	Found concentration (μM)	Recovery (%)	RSD (%) ($n = 3$)
River water	0.1	0.099	99.73	0.220
	1.0	0.995	99.52	0.348
	10	9.893	98.93	0.535
	100	99.17	99.17	0.946
Agricultural soil	0.1	0.099	99.72	0.599
	1.0	0.994	99.46	0.125
	10	9.947	99.47	0.267
	100	98.157	98.15	1.027
Cabbage	0.1	0.098	98.32	0.244
	1.0	0.993	99.30	0.284
	10	9.670	96.70	0.192
	100	97.744	97.74	0.898

polymer thin film was fabricated using a PVA polymer. The synthesis procedure is described in Section 2.4. in the SI. Fig. S12a and b depicts the polymer thin film illuminated under daylight and UV light, respectively. These images reveal that the *M. citrifolia*-CD-based polymer thin film exhibited fluorescence properties with extraordinary photostability, suggesting that the *M. citrifolia*-CDs might be used as fluorescent thin films for smart packaging and solid-state lighting systems.[56] Also, for the fluorescent ink, a refillable pen was filled with the aqueous solution of *M. citrifolia*-CDs and calligraphed CDs on Whatman filter paper.[57] The illuminated text is depicted in Fig. S12c and d in the SI.

3.8. Analytical application of *M. citrifolia*-CDs as a sensor

To explore the real-time application of *M. citrifolia*-CDs to assay clodinafop and cypermethrin, agricultural soil, vegetable (cabbage), and river water samples were evaluated for the practical study. The samples were prepared according to the steps mentioned in the Experimental section. The as-synthesized probe was mixed with the spiked vegetable of various concentrations (0.1, 1.0, 10, and 100 μM) of clodinafop and cypermethrin. The fluorescence data showed a significant change upon the addition of the spiked solution. The found concentrations of clodinafop and cypermethrin were in accordance with the added concentrations, with minute variations due to the complex sample matrix. The recoveries of clodinafop and cypermethrin were found in the ranges of 97.20 to 99.85 and of 96.70 to 99.73%, respectively. The RSD (relative standard deviation) values are in the range of 0.055–0.372 for clodinafop and 0.125–1.027% for cypermethrin, as depicted in Tables 1 and 2. These data suggest that the *M. citrifolia*-CD-based fluorescence approach could be used for assaying clodinafop and cypermethrin in real samples with good reliability and accuracy.

3.9. Blue applicability grade index (BAGI) and ComplexMoGAPI for practicability and sustainability of the developed method

In order to supplement the current green metrics in analytical chemistry, BAGI is recently developed software to assess the feasibility of analytical procedures. The foundation of BAGI is White Analytical Chemistry (WAC), which takes into account three primary perspectives when evaluating methods: practical, analytical, and ecological.[58] The "green" in WAC stands for environmental sustainability, while the "blue" represents economic efficiency and production.[59] By evaluating these characteristics, BAGI produces a pictorial representation that graphically depicts the method's usefulness together with

a score that denotes its applicability.[60] To enable rapid comparisons across various approaches, the scoring system uses a sequential blue color scale to indicate high, medium, low, and no compliance with the requirements. The developed present analytical method for the sensing of clodinafop and cypermethrin using *M. citrifolia*-CDs gives a score of 65.0, suggesting the good practicality of the reported method (Fig. S13a and b in the SI). On the other side, to evaluate the sustainability the ComplexMoGAPI tool was employed. The ComplexMoGAPI tool, a sophisticated variant of the well-known ComplexGAPI first presented by Mansour *et al.* in 2024, is used to evaluate the greenness of our developed method.[61] With a thorough ranking system for each technique ranging from 0 to 100, ComplexMoGAPI provides a notable advance over its predecessor. This technology makes it possible to assess the environmental effects of the developed analytical processes more objectively and quantitatively. The evaluation procedure involves entering the various parameters of the approach into the ComplexMoGAPI program, which is publicly available, and a cumulative greenness score was then produced. The *M. citrifolia*-CD-based fluorescence approach obtains a remarkable greenness score of 85, as depicted in Fig. S14 in the SI. Additionally, using the pulp of *M. citrifolia* makes the method more sustainable and environmentally friendly. Overall, the developed *M. citrifolia*-CD-based fluorescence method could be used as a miniaturized green analytical platform for the detection of clodinafop and cypermethrin in food and environmental samples.

4. Conclusions

Here, *M. citrifolia*-CDs were synthesized using *M. citrifolia* pulp as a rich carbon and heteroatom source *via* the hydrothermal method. When excited at 340 nm, the as-synthesized *M. citrifolia*-CDs showed a characteristic emission peak at 456 nm, displaying blue fluorescence at 365 nm under a UV lamp. The hydrodynamic diameter of the *M. citrifolia*-CDs was found to be 7.17 nm, while the zeta potential value of the *M. citrifolia*-CDs was −37.3 mV. The synthesized *M. citrifolia*-CDs are stable for 100 days and have a quantum yield of 28.92%. The *M. citrifolia*-CD probe is selective for the detection of cypermethrin and clodinafop. Cypermethrin shows quenching in the fluorescence intensity, while clodinafop shows enhancement in the fluorescence intensity. The lifetime analysis shows static quenching in the case of cypermethrin while clodinafop works on the principle of AIE. The FE-TEM images showed the uniformity and dispersed nature of the *M. citrifolia*-CDs with a diameter of 2.0 nm which increased to 9.3 ± 1.4 nm and 11.6 ± 0.8 nm after the addition of pesticides (clodinafop and cypermethrin). The developed *M. citrifolia*-CD-based fluorescence method exhibited good recoveries for the analysis of clodinafop and cypermethrin with LODs of 0.079 and 0.028 μM, respectively, indicating that the developed probe is highly reproducible and sensitive for both pesticide assays. This developed *M. citrifolia*-CD-based fluorescent sensor provides a novel miniaturized analytical platform for selective detection of clodinafop and cypermethrin in various samples, revealing that the integration of *M. citrifolia*-CDs with fluorescence spectrometry is an effective analytical strategy to assay clodinafop and cypermethrin with different spectral variations.

Conflicts of interest

There are no conflicts to declare.

Data availability

The data supporting the findings of this study are available from the corresponding author upon reasonable request.

Supplementary information is available. See DOI: **https://doi.org/10.1039/d5fb00364d**.

Acknowledgements

This work was financially supported by the Gujarat State Biotechnology Mission, Government of Gujarat (Ref. No. GSBTM/JD(R&D)/662/2022-23/00292169, dated 10.03.2023). The authors sincerely acknowledge the Director, SVNIT, Surat, India, for providing the necessary infrastructure to carry out this work.

References

1 M. Motshakeri and H. M. Ghazali, *Trends Food Sci. Techno.*, 2015, **45**, 118–129.
2 J. K. Akanni, L. I. Oduola, G. O. Teslimah and D. E. Olufunmilayo, *American J. Biol. Chem.*, 2019, **7**, 38–46.
3 R. F. Fontes, J. K. Andrade, M. Rajan and N. Narain, *J. Food Sci. Technol.*, 2023, **43**, e103722.
4 P. R. Prasad, A. Z. Visagaperumal and V. Chandy, *Int. J. Pharm. Sci.*, 2019, **2**, 9–20.
5 M. Ali, M. Kenganora and S. N. Manjula, *Pharmacogn. J.*, 2016, **8**, 321–334.
6 N. Oly-Alawuba and A. Iwunze, *Curr. dev. nutr.*, 2019, **3**, nzz034–P10.
7 M. H. Jahurul, C. S. Jack, A. A. Syifa, I. Shahidul, M. R. Norazlina, A. Shihabul and I. S. Zaidul, *Food Chem. Adv*, 2022, **1**, 100079.
8 F. Y. Yusuf, S. V. Atulbhai, B. Swapna, N. I. Malek and S. K. Kailasa, *New J. Chem.*, 2022, **46**, 14287–14308.
9 F. Y. Vadia, V. N. Mehta, S. Jha, T. J. Park, N. I. Malek and S. K. Kailasa, *J. of Fluoresc.*, 2025, **35**, 497–508.
10 S. Moradi, K. Sadrjavadi, N. Farhadian, L. Hosseinzadeh and M. Shahlaei, *J. of Mol. Liq.*, 2018, **259**, 284–290.
11 Y. Liu, H. Huang, W. Cao, B. Mao, Y. Liu and Z. Kang, *Mater. Chem. Front.*, 2020, **4**, 1586–1613.
12 L. Xu, A. M. Abd El-Aty, J. B. Eun, J. H. Shim, J. Zhao, X. Lei, S. Gao, Y. She, F. Jin, J. Wang and M. Jin, *J. Agric. Food Chem.*, 2022, **70**, 13093–13117.
13 N. S. Litoriya, N. R. Chauhan, R. L. Kalasariya, K. D. Parmar, S. Chawla, A. V. Parmar, P. V. Raj and P. G. Shah, *Environ. Sci. Pollut. Res. Int.*, 2023, **30**, 50225–50233.
14 M. Ahemad and M. S. Khan, *Bull. Environ. Contam. Toxicol.*, 2009, **82**, 761–766.

15 K. K. Sikeriya, A. Rawat, P. Mishra and G. Jamliya, *Ann. Plant Soil Res.*, 2023, **25**, 694–696.
16 S. H. Hamada, M. F. Abdel-Lateef, A. E. Abdelmonem, R. M. El-Kholy and A. A. Helalia, *Ann. Agric. Sci.*, 2013, **58**, 13–18.
17 N. Shiry, P. Darvishi, A. Gholamhossieni, P. Pastorino and C. Faggio, *J. Contam. Hydrol.*, 2023, **259**, 104257.
18 V. Sinha and S. Shrivastava, *Indian J. Microbiol.*, 2024, **64**, 48–58.
19 H. Zhao, Y. Zhang, L. Hou, H. Lu, Y. Zhang and M. Xing, *Aquat. Toxicol.*, 2023, **265**, 106760.
20 S. Razzaque, M. Abubakar, M. A. Farid, R. Zia, S. Nazir, H. Razzaque, A. Ali, Z. Ali, A. Mahmood, W. Al-Masry and T. Akhter, *J. of Mater. Chem. B*, 2024, **12**, 9364–9374.
21 R. Kaur and J. Singh, *Nat. Environ. Pollut. Technol.*, 2021, **20**, 1997–2005.
22 S. Mishra, S. S. Patel, S. P. Singh, P. Kumar, M. A. Khan, H. Awasthi and S. Singh, *Environ. Pollut.*, 2022, **310**, 119804.
23 X. Song, F. Li, T. Yan, F. Tian, L. Ren, C. Jiang, Q. Wang and S. Zhang, Process Safety and Environ, *Protection*, 2022, **165**, 610–622.
24 T. Sarkar, H. B. Bohidar and P. R. Solanki, *Int. J. Biol. Macromol.*, 2018, **109**, 687–697.
25 V. Ţucureanu, A. Matei and A. M. Avram, *Crit. Rev. Anal. Chem.*, 2016, **46**, 502–520.
26 B. Wang, S. Wang, Y. Wang, Y. Lv, H. Wu, X. Ma and M. Tan, *Biotechnol. Lett.*, 2016, **38**, 191–201.
27 Y. Dai, Z. Liu, Y. Bai, Z. Chen, J. Qin and F. Feng, *RSC adv.*, 2018, **8**, 42246–42252.
28 H. Zhang, L. Zhao, F. Geng, L. H. Guo, B. Wan and Y. Yang, *Appl. Catal. B: Environ.*, 2016, **180**, 656–662.
29 F. Fiori, H. Moukham, F. Olia, D. Piras, S. Ledda, A. Salis, L. Stagi, L. Malfatti and P. Innocenzi, *Mater*, 2022, **15**, 2395.
30 J. Yu, C. Liu, K. Yuan, Z. Lu, Y. Cheng, L. Li, X. Zhang, P. Jin, F. Meng and H. Liu, *Nanomater.*, 2018, **8**, 233.
31 R. Atchudan, P. Gangadaran, S. Perumal, T. N. Edison, A. K. Sundramoorthy, R. L. Rajendran, B. C. Ahn and Y. R. Lee, *J. Clust. Sci.*, 2023, **34**, 1583–1594.
32 V. Arul and M. G. Sethuraman, *Opt. Mater.*, 2018, **78**, 181–190.
33 S. Durrani, J. Zhang, Z. Yang, A. P. Pang, J. Zeng, S. M. Sayed, A. Khan, Y. Zhang, F. G. Wu and F. Lin, *Anal. Chim. Acta*, 2022, **1202**, 339672.
34 F. Y. Vadia, V. N. Mehta, S. Jha, T. J. Park, N. I. Malek and S. K. Kailasa, *J. Fluoresc.*, 2025, **35**, 497–508.
35 S. Ghosh, A. R. Gul, C. Y. Park, M. W. Kim, P. Xu, S. H. Baek, J. R. Bhamore, S. K. Kailasa and T. J. Park, *Chemosphere*, 2021, **279**, 130515.
36 J. Zhao, F. Li, S. Zhang, Y. An and S. Sun, *New J. Chem.*, 2019, **43**, 6332–6342.
37 R. R. Anjana, J. S. Anjali Devi, M. Jayasree, R. S. Aparna, B. Aswathy, G. L. Praveen, G. M. Lekha and G. S. Sony, *Microchim. Acta*, 2018, **185**, 1.
38 M. Bhatt, S. Bhatt, G. Vyas, I. H. Raval, S. Haldar and P. Paul, *ACS Appl. Nano Maters.*, 2020, **3**, 7096–7104.
39 E. Ciotta, P. Prosposito and R. Pizzoferrato, *J. Lumin.*, 2019, **206**, 518–522.
40 F. Y. Vadia, N. I. Malek and S. K. Kailasa, *J. Fluoresc.*, 2025, **35**, 5345–5354.
41 M. Rezaee and F. Khalilian, *J. Anal. Chem.*, 2024, **79**, 540–545.
42 N. Li, D. Han, X. Ma, C. Qiu, Y. Qin, T. Yao, S. Wang, Y. She, F. Hacımüftüoğlu and A. M. Abd El-Aty, *Biomed. Chromatogr.*, 2022, **36**, e5303.
43 J. Duan, M. Wang, M. Sun, W. Wu, B. Hu and T. Gao, *Chin. J. Pestic. Sci.*, 2013, **15**, 121–124.
44 K. U. Jaffar, A. U. Kakar, M. Asghar, S. Khan and N. Khan, *Int. J. Environ. Anal. Chem.*, 2024, **1–21**, DOI: **10.1080/03067319.2024.2416516**.
45 H. Bagheri, S. Asgari and H. Piri-Moghadam, *Chromatographia*, 2014, **77**, 723–728.
46 N. G. Vajubhai, P. Chetti and S. K. Kailasa, *ACS Appl. Nano Mater.*, 2022, **5**, 18220–18228.
47 Y. Li, L. Zhang, Y. Dang, Z. Chen, R. Zhang, Y. Li and B. C. Ye, *Biosens. Bioelectron.*, 2019, **127**, 207–214.
48 Y. Wang, M. Wang, X. Sun, G. Shi, J. Zhang, W. Ma and L. Ren, *Opt. Express*, 2018, **26**, 22168–22181.
49 Y. Zhao, X. Ruan, Y. Song, J. N. Smith, N. Vasylieva, B. D. Hammock, Y. Lin and D. Du, *Anal. chem.*, 2021, **93**, 13658–13666.
50 H. J. Lee, G. Shan, K. C. Ahn, E. K. Park, T. Watanabe, S. J. Gee and B. D. Hammock, *J. Agric. Food Chem.*, 2004, **52**, 1039–1043.
51 F. Abdi, K. A. Dilmaghani and R. Mohammadi, *J. Ind. Eng. Chem.*, 2025, DOI: **10.1016/j.jiec.2025.06.036**.
52 W. Leung, S. Limwichean, N. Nuntawong, P. Eiamchai, S. Kalasung, O. U. Nimittrakoolchai and N. Houngkamhang, *Eng. Mater.*, 2020, **853**, 102–106.
53 M. Muhammad, S. Khan, G. Rahim, W. Alharbi and K. H. Alharbi, *Environ. Monit. Assess.*, 2022, **194**, 1–9.
54 S. Nayak, S. Borse, S. Jha, V. N. Mehta, Z. V. Murthy, T. J. Park and S. K. Kailasa, *J. Fluoresc.*, 2025, **35**, 509–520.
55 S. S. Arumugam, J. Xuing, A. Viswadevarayalu, Y. Rong, D. Sabarinathan, S. Ali, A. A. Agyekum, H. Li and Q. Chen, *J. Photochem. Photobiol. A.*, 2020, **401**, 112788.
56 J. Shen, H. Gu, Z. He and W. Lin, *Ind. Eng. Chem. Res.*, 2023, **62**, 3622–3634.
57 B. Zhang, Y. Luo, B. Peng, L. Zhang, N. Xie, D. Yue, W. Li, B. Qin, W. Du, Z. Wang and Y. Zhang, *J. Mol. Struct.*, 2024, **1304**, 137739.
58 P. M. Nowak, R. Wietecha-Posłuszny and J. Pawliszyn, *TrAC Trends Anal. Chem.*, 2021, **138**, 116223.
59 T. A. Zughaibi and A. I. Al-Asmari, *Green Anal. Chem.*, 2025, **12**, 100178.
60 N. Manousi, W. Wojnowski, J. Płotka-Wasylka and V. Samanidou, *Green chem.*, 2023, **25**, 7598–7604.
61 F. R. Mansour, K. M. Omer and J. Płotka-Wasylka, *Green Anal. Chem.*, 2024, **10**, 100126.